THE JOURNAL OF BIOLOGICAL CHEMISTRY VOL. 284, NO. 21, pp. 14558–14571, May 22, 2009

Lysophosphatidic Acid 2 Receptor-mediated Supramolecular Complex Formation Regulates Its Antiapoptotic Effect*[S]

Received for publication, January 9, 2009, and in revised form, February 23, 2009 Published, JBC Papers in Press, March 17, 2009, DOI 10.1074/jbc.M900185200

Shuyu E[‡1], Yun-Ju Lai[§1], Ryoko Tsukahara[‡], Chen-Shan Chen[§], Yuko Fujiwara[‡], Junming Yue[‡], Jei-Hwa Yu[¶], Huazhang Guo[‡], Akio Kihara[‖], Gábor Tigyi[‡2], and Fang-Tsyr Lin[§3]

From the [‡]Department of Physiology, University of Tennessee Health Science Center, Memphis, Tennessee 38163, the Departments of [§]Cell Biology and [¶]Biochemistry and Molecular Genetics, University of Alabama at Birmingham, Birmingham, Alabama 35294, and the [‖]Laboratory of Biomembrane and Biofunctional Chemistry, Faculty of Pharmaceutical Sciences, Hokkaido University, Kita 12-jo, Nishi 6-choume, Kita-ku, Sapporo 060-0812, Japan

The G protein-coupled lysophosphatidic acid 2 (LPA_2) receptor elicits prosurvival responses to prevent and rescue cells from apoptosis. However, G protein-coupled signals are not sufficient for the full protective effect of LPA_2. LPA_2 differs from other LPA receptor subtypes in the C-terminal tail, where it contains a zinc finger-binding motif for the interactions with LIM domain-containing TRIP6 and proapoptotic Siva-1, and a PDZ-binding motif through which it complexes with the NHERF2 scaffold protein. In this report, we identify a unique C*XX*C motif of LPA_2 responsible for the binding to TRIP6 and Siva-1, and demonstrate that disruption of these macromolecular complexes or knockdown of TRIP6 or NHERF2 expression attenuates LPA_2-mediated protection from chemotherapeutic agent-induced apoptosis. In contrast, knockdown of Siva-1 expression enhances this effect. Furthermore, a PDZ-mediated direct interaction between TRIP6 and NHERF2 facilitates their interaction with LPA_2. Together, these results suggest that in addition to G protein-activated signals, the cooperation embedded in the LPA_2-TRIP6-NHERF2 ternary complex provides a novel ligand-dependent signal amplification mechanism that is required for LPA_2-mediated full activation of antiapoptotic signaling.

Lysophosphatidic acid (LPA)[4] is a growth factor-like lysophospholipid abundantly present in biological fluids. It mediates diverse cellular responses important for cell survival, growth, differentiation, migration, inflammation, angiogenesis, and platelet aggregation (1, 2). At least eight G protein-coupled LPA receptors have been identified: LPA_1, LPA_2, and LPA_3 of the endothelial differentiation gene family and the structurally distinct LPA_4/P2Y9, LPA_5/GPR92, LPA_6/GPR87, LPA_7/P2Y5, and LPA_8/P2Y10 of the purinergic receptor cluster (3–5). These receptors couple to $G_{i/o}$, $G_{q/11}$, G_s, and/or $G_{12/13}$ proteins to activate various signaling pathways. However, the molecular mechanisms underlying the specificity and diversity with which different LPA receptors regulate these wide ranging cellular responses are not yet fully understood.

Substantial evidence has demonstrated that LPA is a survival factor that protects non-transformed cells from different stress-induced apoptosis (6) and renders cancer cells resistance to apoptosis-inducing treatments (1, 2). Among the various G protein-coupled LPA receptors, LPA_2 has been shown to mediate the antiapoptotic effect of LPA *in vivo*. $LPA_2^{-/-}$ mice show significantly increased rates of radiation-induced apoptosis and less crypt survival (7). LPA protects gut epithelial cells from radiation-induced apoptosis in WT and $LPA_1^{-/-}$ mice but not in $LPA_2^{-/-}$ mice (7). The classical paradigm for G protein-coupled receptor (GPCR)-mediated prosurvival signaling involves the coupling of ligand-bound receptors to heterotrimeric G proteins that sequentially activate the downstream effectors involved in Ras/ERK, phosphatidylinositol 3-kinase (PI3K)/AKT, and NF-κB signaling pathways (6). However, recent evidence suggests that non-G protein-coupled signals mediated via the unique C-terminal binding motifs of LPA_2 may be required for its antiapoptotic function. LPA_2 is the only LPA receptor subtype known to interact with various molecules via the unique binding domains present in its C terminus (8). The last four amino acids, DSTL, of LPA_2 bind to several PDZ proteins, including NHERF2 (Na^+/H^+ exchanger regulatory factor), PDZ-RhoGEF, LARG (leukemia-associated RhoGEF), and MAGI-3 (membrane-associated guanylate kinase with an inverted domain structure-3) (9–13). These scaffold proteins modulate LPA-induced activation of ERK and/or RhoA. NHERF2 can also regulate phospholipase C-β3 signaling pathways and bridge LPA_2 to cystic fibrosis transmembrane regulator Cl^- channel (9, 10). Through the PDZ-mediated interactions, membrane-localized NHERF2 and MAGI-3 can recruit the phosphatase and tensin homolog in close proximity to the cell surface to restrict PI3K/

* This work was supported, in whole or in part, by National Institutes of Health Grants CA92160 (to G. T.), AI 080405 (to G. T.), and CA100848 (to F. L.). This work was also supported by a grant from the Marsha Rivkin Center for Ovarian Cancer Research (to F. L.). G. T. is a founder of RxBio Inc. and a member of the scientific advisory board.

[S] The on-line version of this article (available at http://www.jbc.org) contains supplemental Figs. S1–S4.

[1] Both authors contributed equally to this work.

[2] To whom correspondence may be addressed. Tel.: 901-448-4793; Fax: 901-448-7126; E-mail: gtigyi@physio1.utmem.edu.

[3] To whom correspondence may be addressed. Tel.: 205-975-5060; Fax: 205-975-5648; E-mail: flin@uab.edu.

[4] The abbreviations used are: LPA, lysophosphatidic acid; GPCR, G protein-coupled receptor; 2-BP, 2-bromopalmitate; ERK, extracellular signal-regulated kinase; PI3K, phosphatidylinositol 3-kinase; WT, wild type; siRNA, small interfering RNA; BSA, bovine serum albumin; DMEM, Dulbecco's modified Eagle's medium; PTX, pertussis toxin; MEF, mouse embryonic fibroblast; DKO, double knock-out; S1P, sphingosine 1-phosphate; GFP, green fluorescent protein.

AKT activity (14, 15). However, NHERF2 can also serve as a scaffold protein for PDK1 (3-phosphoinositide-dependent protein kinase 1), which plays a central role in the activation of AGC family kinases, including AKT (16). It has been reported that knockdown of NHERF2 attenuates LPA-induced AKT activation in colon cancer cells (12). Thus, the function of NHERF2 in restricting or promoting PI3K/AKT signaling may depend on the relative cellular expression levels of phosphatase and tensin homolog *versus* PDK1.

Two zinc finger proteins, including the LIM domain-containing TRIP6 and Siva-1 proapoptotic protein, have been found to bind to the C-terminal tail of LPA$_2$ (17, 18). The LIM domain is comprised of two zinc finger motifs, which are critical for protein-protein interactions (19). The association of TRIP6 with LPA$_2$ enhances LPA-induced ERK activation and cell migration in a c-Src-dependent manner (20). However, it is unknown whether TRIP6 plays any role in the LPA$_2$-mediated antiapoptotic effect. In contrast, Siva-1, a transcriptional target of p53 and E2F1, functions as a proapoptotic protein during DNA damage response (21). The binding of LPA$_2$ to Siva-1 promotes LPA-dependent ubiquitination and down-regulation of Siva-1 expression (18).

As different LPA receptors show overlapping patterns of G protein coupling, LPA$_2$-mediated protein-protein interactions may be particularly important in the signal amplification and diversification of this receptor subtype. Here we demonstrate that an LPA-induced ternary complex of TRIP6 NHERF2 and LPA$_2$ regulates antiapoptotic function. We have mapped the C*XX*C zinc finger-binding motif of LPA$_2$ and found the LPA$_2$-mediated antiapoptotic effect was abolished only when both C*XX*C- and PDZ-binding motifs were disrupted, indicating that the supramolecular complexes formed via the C-terminal tail of LPA$_2$ are required for the full antiapoptotic function of LPA$_2$, and thus play a critical role in the chemoprotective action of LPA in cancer cells.

EXPERIMENTAL PROCEDURES

Plasmid Construction and Site-directed Mutagenesis—The cDNA sequences encoding one of the deletion mutants or point mutants of FLAG-LPA$_2$ were amplified by overlapping extension PCR and inserted into pcDNA3.1 (Invitrogen). These cDNA fragments were subsequently subcloned into pcFUW-puro lentiviral vector. The cDNA sequences encoding full-length NEHRF2, NHERF-PDZ1 (residues 8–99), or NHERF2-PDZ2 (residues 149–228) were inserted in-frame into pEGFP (Clontech) or pGEX-6P3 (Amersham Biosciences). The full-length TRIP6 cDNA sequences were inserted in-frame into pEBFP-C1. The expression vectors of GST-LPA$_2$-CT mutants in which Cys-311 and/or Cys-314 were mutated to Ala were constructed by

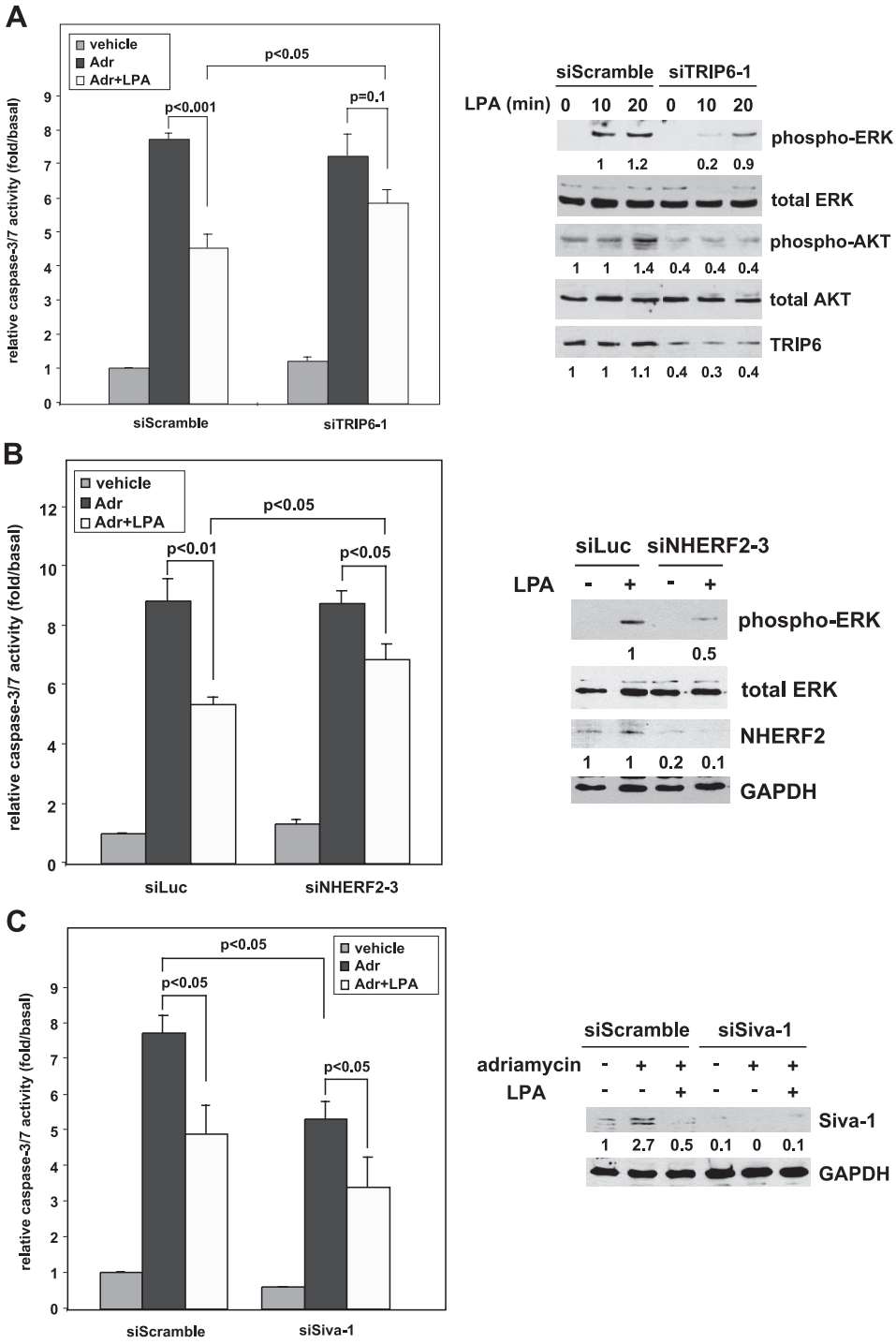

QuikChange site-directed mutagenesis (Stratagene) using pGEX-6P1-LPA$_2$-CT (17) as the template. The pLVTHM (Addgene) lentiviral vector was used to direct the expression of a short hairpin RNA that specifically targets the 19-nucleotide sequences of mouse TRIP6 (siTRIP6-1) (20), human TRIP6 (siTRIP6-2, siTRIP6-3) (17), mouse Siva-1 (18), or human NHERF2 cDNA (siNHERF2-4 (10) and siNHERF2-5, 5′-CCTGCATAGTGACAAGTCC-3′), respectively. The pGIPZ lentiviral expression vector (Openbiosystems) was used to direct the expression of a miR-30-based mouse NHERF2 short hairpin RNA (siNHERF2-3) or a luciferase control short hairpin RNA, which specifically targets the 22-nucleotide sequences of mouse NHERF2 cDNA (5′-ATCAGAGAAGGACAATGAGGAT-3′) and luciferase cDNA (5′-CCACTTACGCTGAGTACTTCGA-3′), respectively. pCMV-FLAG-ΔTTDC was constructed by deleting the cDNAs encoding the distal four amino acids, TTDC, of TRIP6 using QuikChange site-directed mutagenesis (Stratagene). All of these cDNA constructs have been verified by DNA sequencing.

Stable Transfection—Primary mouse embryonic fibroblasts (MEF) were isolated from E13.5 LPA$_{1/2}$ DKO embryos and continuously cultured to obtain the spontaneously immortalized MEF cell lines. These MEFs were transduced with an empty lentivirus or the lentivirus harboring WT or one of the FLAG-LPA$_2$ mutants and selected with puromycin to establish the stable cell lines.

Cellular Co-immunoprecipitation, In Vitro Binding, Immunoblotting, Immunostaining, and LPA-induced Calcium Activation Assay—Experiments and purification of the recombinant Siva-1 and TRIP6 were performed as described previously (7, 17, 18, 20). To detect the interactions of LPA$_2$, NHERF2, and TRIP6 at physiological levels, SKOV-3 cells expressing a scrambled siRNA, a TRIP6 siRNA, or a NHERF2 siRNA were starved in 0.1% fatty acid-free bovine serum albumin (BSA)-containing DMEM overnight, followed by addition of 2 μM LPA for 10 min and harvested. Endogenous LPA$_2$ was immunoprecipitated with an anti-LPA$_2$ rat antibody (a gift from Dr. Junken Aoki) or a control rat IgG. TRIP6 was immunoprecipitated with an anti-TRIP6 mouse monoclonal antibody (BD Biosciences) or a control mouse IgG. Proteins were resolved by SDS-PAGE and subjected to immunoblotting using an antibody specific to NHERF2, LPA$_2$ (gifts from Dr. A. P. Naren), or TRIP6 (Bethyl Laboratories), respectively.

Palmitoylation of LPA$_2$—HEK 293T cells expressing WT or one of the point mutants of FLAG-LPA$_2$ were incubated with [^{3}H]palmitic acid (60 Ci/mmol, Amersham Biosciences) at 37 °C for 2 h. FLAG-LPA$_2$ in the whole cell lysates was immunoprecipitated with the anti-FLAG M2 monoclonal antibody-conjugated agarose beads, resolved by SDS-PAGE, and detected by autoradiography. The blot was then probed with an anti-FLAG antibody to detect FLAG-LPA$_2$. The effect of 2-bromopalmitate (2-BP, Sigma) on the inhibition of LPA$_2$ palmitoylation was determined by pretreating the transfected HEK 293T cells with 100 μM 2-bromopalmitate for 30 min followed by labeling with [^{3}H]palmitic acid.

To determine whether inhibition of palmitoylation affects LPA$_2$ binding to Siva-1, TRIP6, or NHERF2, HEK 293T cells transiently expressing GFP-Siva-1, GFP-TRIP6, or GFP-NHERF2 with or without FLAG-LPA$_2$ were pretreated with 100 μM 2-BP in 0.1% fatty acid-free BSA-containing DMEM for 4 h, followed by addition of 2 μM LPA for 10 min. After immunoprecipitation of FLAG-LPA$_2$, half the precipitates were resolved by SDS-PAGE. Immunoblotting was performed to detect the co-immunoprecipitated GFP-Siva-1, GFP-TRIP6, or GFP-NHERF2. The rest of the samples were subjected to the acyl-biotinyl exchange procedure (22) to determine the levels of palmitoylated LPA$_2$. Precipitated LPA$_2$ was pretreated with 50 mM *N*-ethylmaleimide (Pierce) for 1 h, followed by the acyl-biotinyl exchange with 1 M hydroxylamine and 0.2 mM EZ-link biotin-*N*-[6-(biotinamido)hexyl]-3′-(2′-pyridyldithio)propionamide (HPDP) (Pierce) for another hour at room temperature. Biotinylated FLAG-LPA$_2$ was eluted from the anti-FLAG beads using 100 μg/ml FLAG peptides (Sigma) for competition and subsequently pulled down with avidin beads (Amersham Biosciences). After SDS-PAGE, immunoblotting was performed using an anti-FLAG rabbit polyclonal antibody (Sigma).

Apoptosis Assays—Stable MEFs were starved in 0.1% fatty acid-free BSA-containing DMEM with or without 10 μM LPA for 1 h followed by the addition of 1.5 to 2 μM adriamycin for 7–9 h. Caspase-3/7 activity was determined by cleavage of the luminogenic substrate containing the DEVD sequence (Promega) and was normalized by protein concentrations. To determine the effect of pertussis toxin (PTX) on apoptosis, DKO-LPA$_2$ MEFs were pretreated with 100 ng/ml PTX overnight before the apoptosis assay. Alternatively,

FIGURE 1. **LPA$_2$-mediated protection from adriamycin-induced apoptosis is regulated by proteins interacting with its C-terminal tail.** *A*, knockdown of TRIP6 expression reduces LPA$_2$-mediated ERK and AKT activation and protection from adriamycin-induced caspase-3/7 activation. LPA$_{1/2}$ DKO MEFs stably expressing FLAG-LPA$_2$ (*DKO-LPA$_2$*) were transduced with the lentivirus harboring a mouse TRIP6 siRNA (*siTRIP6-1*) or a scrambled control siRNA (*siScramble*). After starvation for 4 h, cells were treated with 2 μM LPA for 10 or 20 min, and immunoblotting was performed to determine the levels of activated phospho-ERK or phospho-AKT, respectively (*right panel*). The same blot was reprobed with an antibody specific to ERK, AKT, or TRIP6, respectively. The intensity of each protein was quantified by NIH IMAGE J software and the relative expression of phospho-ERK or phospho-AKT was normalized by the levels of total ERK or AKT. The same cells were starved in 0.1% fatty acid-free BSA-containing DMEM with or without 10 μM LPA for 1 h followed by the addition of 1.7 μM adriamcyin for 9 h, and caspase-3/7 activity was determined by cleavage of the luminogenic substrate containing the DEVD sequence and was normalized by protein concentrations (*left panel*). Data shown are the mean ± S.E. of five independent experiments. Statistic significance ($p < 0.05$) was determined by Student's *t* test. *B*, knockdown of NHERF2 expression attenuates LPA$_2$-mediated ERK activation and protection from adriamycin-induced apoptosis. DKO-LPA$_2$ MEFs were transduced with the lentivirus harboring a mouse NHERF2 siRNA (*siNHERF2-3*) or a luciferase control siRNA (*siLuc*). The starved cells were treated with LPA for 10 min and the levels of activated ERK, total ERK, NHERF2, and glyceraldehyde-3-phosphate dehydrogenase (*GAPDH*) in the whole cell lysates were determined by immunoblotting. Adriamycin-induced caspase-3/7 activation were assayed as described in *A*. Data shown are the mean ± S.E. of three independent experiments. *C*, inhibition of Siva-1 expression enhances LPA$_2$-mediated protection from adriamycin-induced apoptosis. DKO-LPA$_2$ MEFs were transduced with the lentivirus harboring a Siva-1 siRNA or a scrambled siRNA. The effect of LPA on adriamycin-induced caspase-3/7 activation was determined as described in *A*. Data shown are the mean ± S.E. of three independent experiments. Immunoblotting was performed to detect the expression of Siva-1 and control GAPDH in the whole cell lysates.

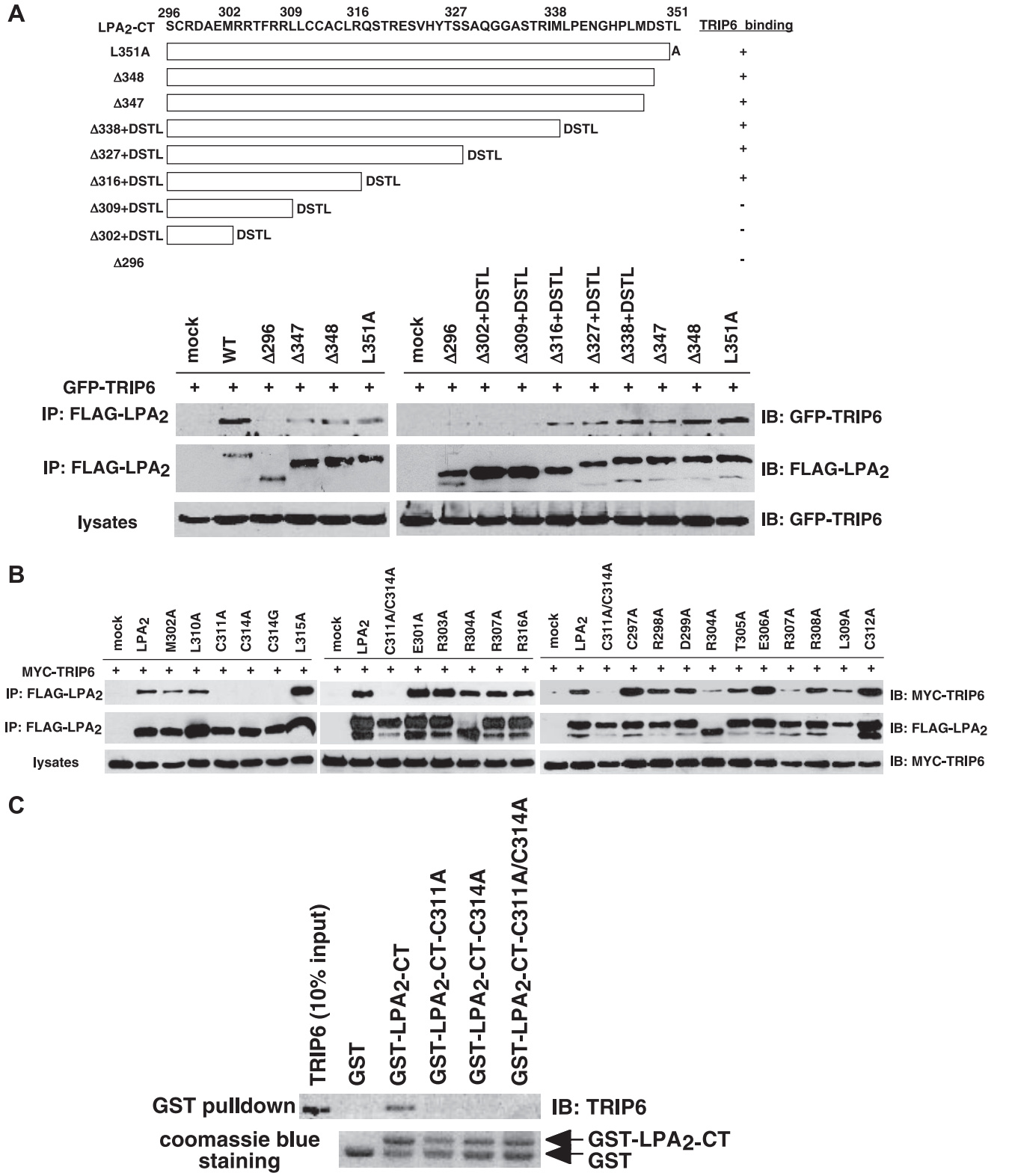

FIGURE 2. **The ^{311}*CXXC*^{314} motif of LPA$_2$ is required for the interaction with TRIP6.** *A*, the TRIP6-binding motif of LPA$_2$ is located in the region proximal to Arg-316 of the C-terminal tail. GFP-TRIP6 was expressed in HEK 293T cells with FLAG-LPA$_2$ or one of the LPA$_2$ deletion mutants with or without the DSTL sequences as indicated in the *top panel*. After stimulation of the cells with 2 μM LPA for 10 min, LPA$_2$ was immunoprecipitated (*IP*) with anti-FLAG M2 antibody-conjugated agarose beads and resolved by SDS-PAGE. GFP-TRIP6 co-immunoprecipitated with LPA$_2$ was detected by immunoblotting (*IB*) using an anti-GFP antibody. *B*, the ability of LPA$_2$ to bind to TRIP6 is eliminated by mutation of Cys-311 and/or Cys-314 to Ala. MYC-TRIP6 was co-expressed with WT or one of the point mutants of LPA$_2$ in HEK 293T cells. Co-immunoprecipitation was performed as described above. MYC-TRIP6 co-immunoprecipitated with LPA$_2$ was detected with an anti-MYC polyclonal antibody. *C*, Cys-311 or Cys-314 of LPA$_2$ mediates the binding to TRIP6 *in vitro*. Purified recombinant TRIP6 was incubated with glutathione *S*-transferase (*GST*), GST-LPA$_2$-CT, or one of the GST-LPA$_2$-CT mutants at 4 °C for 3 h. TRIP6 pulled down by GST-LPA$_2$-CT was resolved by SDS-PAGE and detected by immunoblotting using an anti-TRIP6 antibody. The *bottom panel* shows Coomassie Blue staining of GST and GST-LPA$_2$-CT proteins. Data shown in each figure are representative of three independent experiments.

apoptosis was determined by annexin V-fluorescein isothiocyanate staining (BD Biosciences) and analyzed by flow cytometry following a 14-h treatment. SKOV-3 cells transduced with the lentivirus harboring a scrambled siRNA, TRIP6 siRNA, or a NHERF2 siRNA were starved and pretreated with LPA followed by the addition of 50 μM cisplatin for 20 h. Apoptosis was determined by caspase-3/7 activity assay and immunoblotting using an antibody specific to PARP-1 (BD Biosciences).

To determine apoptosis by DNA fragmentation assay, stable MEFs were seeded on plates coated with 0.1 mg/ml poly-L-lysine overnight followed by the addition of 3 μM adriamycin in 0.5% fetal bovine serum-containing DMEM. Two μM LPA were added 1 h later. After a 6-h treatment, DNA fragmentation was measured by enzyme-linked immunosorbent assay following the procedure of the Cell Death Detection Kit (Roche).

Statistic Analysis—Statistic significance ($p < 0.05$) was determined using Student's *t* test.

RESULTS

LPA$_2$-mediated Protection from Chemotherapeutic Agent-induced Apoptosis Is Regulated by Proteins Interacting with the C terminus of LPA$_2$—To elucidate the unique properties of LPA$_2$ leading to the attenuation of DNA damage-induced apoptosis, we tested the hypothesis that LPA$_2$-elicited antiapoptotic signaling could be regulated through the interactions with its C terminus-binding partners. We knocked down the expression of TRIP6, NHERF2, or Siva-1 in LPA$_{1/2}$ double knock-out (DKO) MEFs stably transduced with a human LPA$_2$ (designated DKO-LPA$_2$ MEFs). These LPA$_{1/2}$ DKO MEFs were chosen because LPA fails to induce ERK/AKT activation in these MEFs required for the antiapoptotic effect (Fig. 5*C*), and cannot protect them from

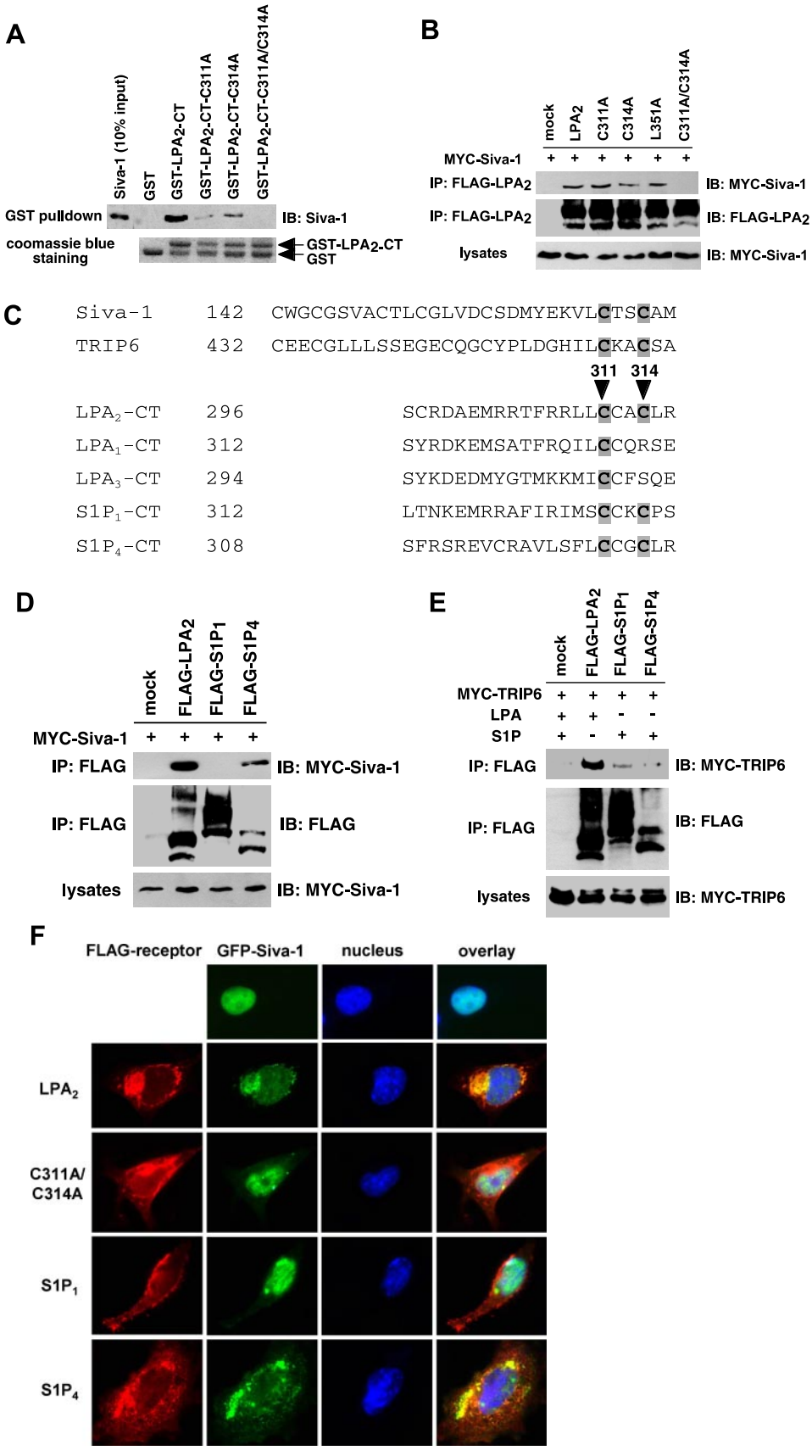

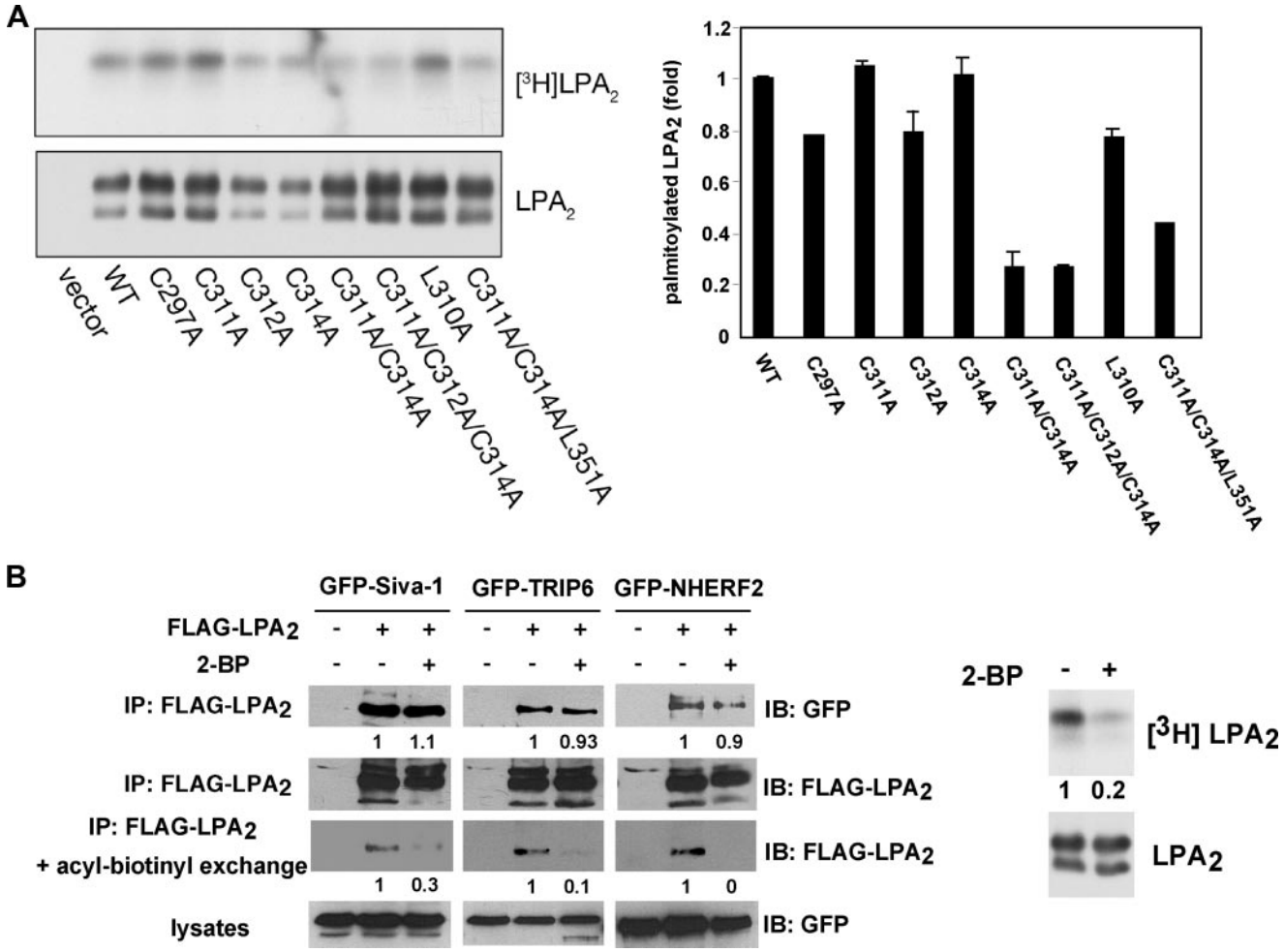

FIGURE 4. **Palmitoylation modification does not affect LPA$_2$ binding to TRIP6, Siva-1, or NHERF2.** *A*, palmitoylation of LPA$_2$ is partially impaired by mutation of the cysteine residues in the proximal end of its C-terminal tail. WT or one of the point mutants of FLAG-LPA$_2$ were transiently expressed in HEK 293T cells and labeled with [^{3}H]palmitic acid at 37 °C for 2 h. FLAG-LPA$_2$ was immunoprecipitated with anti-FLAG M2 monoclonal antibody-conjugated agarose beads, resolved by SDS-PAGE, and detected by autoradiography (*left top panel*), followed by immunoblotting (*IB*) with an anti-FLAG antibody (*left bottom panel*). The *right panel* shows the relative levels of palmitoylation of each mutant compared with WT LPA$_2$ after normalization by total receptor expression. Data shown are the mean of two to three independent experiments. *B*, association of LPA$_2$ with Siva-1, TRIP6, or NHERF2 is not affected by blocking palmitoylation of LPA$_2$. GFP-Siva-1, GFP-TRIP6, or GFP-NHERF2 was co-expressed with FLAG-LPA$_2$ in HEK 293T cells. After treatment with 100 μM 2-BP in 0.1% fatty acid-free BSA-containing DMEM for 4 h, cells were stimulated with LPA for 10 min and FLAG-LPA$_2$ was immunoprecipitated with anti-FLAG M2 monoclonal antibody-conjugated agarose beads. Half the precipitates were resolved by SDS-PAGE and the immunoblot (*IB*) was probed with an anti-GFP polyclonal antibody to detect co-immunoprecipitated GFP-Siva-1, GFP-TRIP6, or GFP-NHERF2. The rest of the samples were subjected to the acyl-biotinyl exchange procedure to determine levels of palmitoylated LPA$_2$ as described under "Experimental Procedures." A separate experiment was performed to determine the effect of 2-BP on blocking palmitoylation of LPA$_2$ by pretreating the FLAG-LPA$_2$-expressing HEK 293T cells with 100 μM 2-BP for 30 min followed by labeling with [^{3}H]palmitic acid for 2 h (*right panel*). The relative levels of Siva-1, TRIP6, or NHERF2 co-immunoprecipitated (*IP*) with FLAG-LPA$_2$ were quantified and normalized to the levels of FLAG-LPA$_2$ immunoprecipitates. Data shown are representative of three separate experiments.

adriamycin-induced apoptosis (Fig. 5*D*), although they endogenously express LPA$_4$ and LPA$_7$ receptor transcripts (data not shown). We found that 60% knockdown of TRIP6 expression did not further enhance adriamycin-induced caspase-3/7 activation but significantly attenuated LPA-mediated protection and the activation of ERK and AKT (Fig.

FIGURE 3. **Both Cys-311 and Cys-314 residues are required for LPA$_2$ binding to Siva-1.** *A*, *in vitro* binding of LPA$_2$ to Siva-1 is partially impaired by mutation of Cys-311 or Cys-314 to Ala and is completely abolished when both cysteine residues are mutated. Purified recombinant Siva-1 was incubated with glutathione *S*-transferase (*GST*), GST-LPA$_2$-CT, or one of the GST-LPA$_2$-CT mutants. Siva-1 pulled down by GST-LPA$_2$-CT was detected by immunoblotting using an anti-Siva-1 antibody. *B*, association of LPA$_2$ with Siva-1 is eliminated only when both Cys-311 and Cys-314 residues are mutated to Ala. MYC-Siva-1 was co-expressed with WT or one of the point mutants of FLAG-LPA$_2$ in HEK 293T cells. Cells were starved overnight and then harvested for co-immunoprecipitation (*IP*) and immunoblotting (*IB*) as described above. MYC-Siva-1 was detected with an anti-MYC polyclonal antibody. *C*, amino acid sequence alignment of the C-terminal zinc finger of Siva-1 (residues 142–172) and TRIP6-LIM3 (residues 432–462), and the proximal region of the C-terminal tail of LPA$_2$ (residues 296–316), LPA$_1$ (residues 312–332), LPA$_3$ (residues 294–314), S1P$_1$ (residues 312–322), and S1P$_4$ (residues 308–318). *D*, Siva-1 interacts with S1P$_4$ but not S1P$_1$. HEK 293T cells expressing MYC-Siva-1 with FLAG-tagged LPA$_2$, S1P$_1$, or S1P$_4$ were subjected to a co-immunoprecipitation experiment as described in *B*. *E*, TRIP6 binds weakly to S1P$_1$ and barely associates with S1P$_4$. HEK 293T cells expressing MYC-TRIP6 with FLAG-tagged LPA$_2$, S1P$_1$, or S1P$_4$ were starved for 8 h followed by the addition of 2 μM LPA or S1P for 10 min. Co-immunoprecipitation was performed as described above. Data shown in *A*, *B*, *D*, and *E* are representative of three independent experiments. *F*, Siva-1 colocalizes with LPA$_2$ and S1P$_4$ but not S1P$_1$ or the C311A/C314A mutant of LPA$_2$ in the cytosol. GFP-Siva-1 was transiently co-expressed with FLAG-tagged LPA$_2$, C311A/C314A of LPA$_2$, S1P$_1$, or S1P$_4$ in LPA$_{1/2}$ DKO MEFs. Cells were fixed, permeabilized, and then incubated with the anti-FLAG M2 monoclonal antibody followed by the Texas Red X-conjugated mouse secondary antibody to detect the FLAG-tagged receptors. GFP-Siva-1 was directly visualized by fluorescence microscopy.

1*A*). Knockdown of NHERF2 expression by 80% also reduced LPA-induced chemoprotection and ERK activation (Fig. 1*B*). In contrast, knockdown of Siva-1 expression by more than 90% reduced adriamycin-induced caspase-3/7 activation and enhanced the LPA-mediated protective effect (Fig. 1*C*). These results suggest that in mouse embryonic fibroblasts, the antiapoptotic effect of LPA_2 involves NHERF2, TRIP6, and Siva-1.

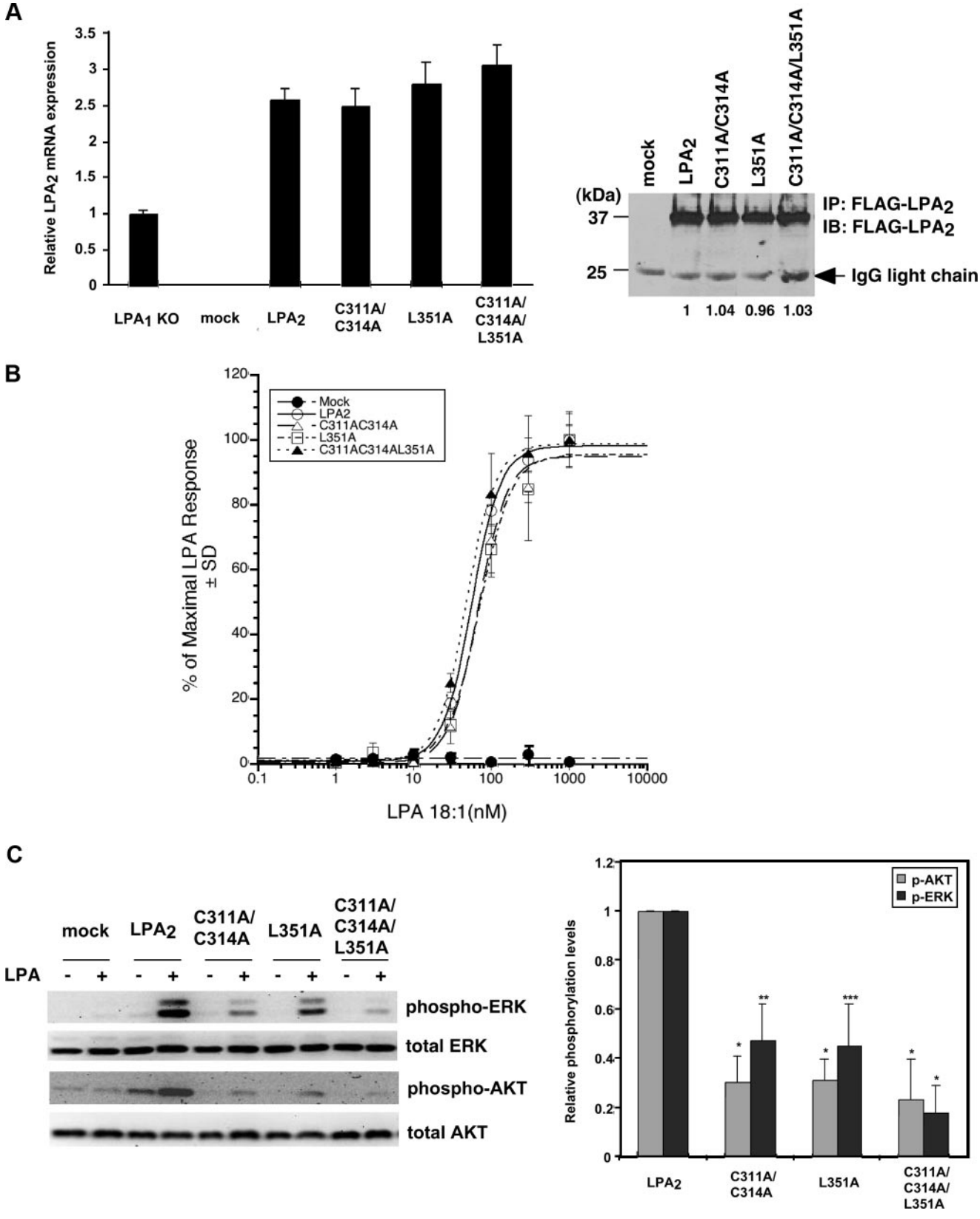

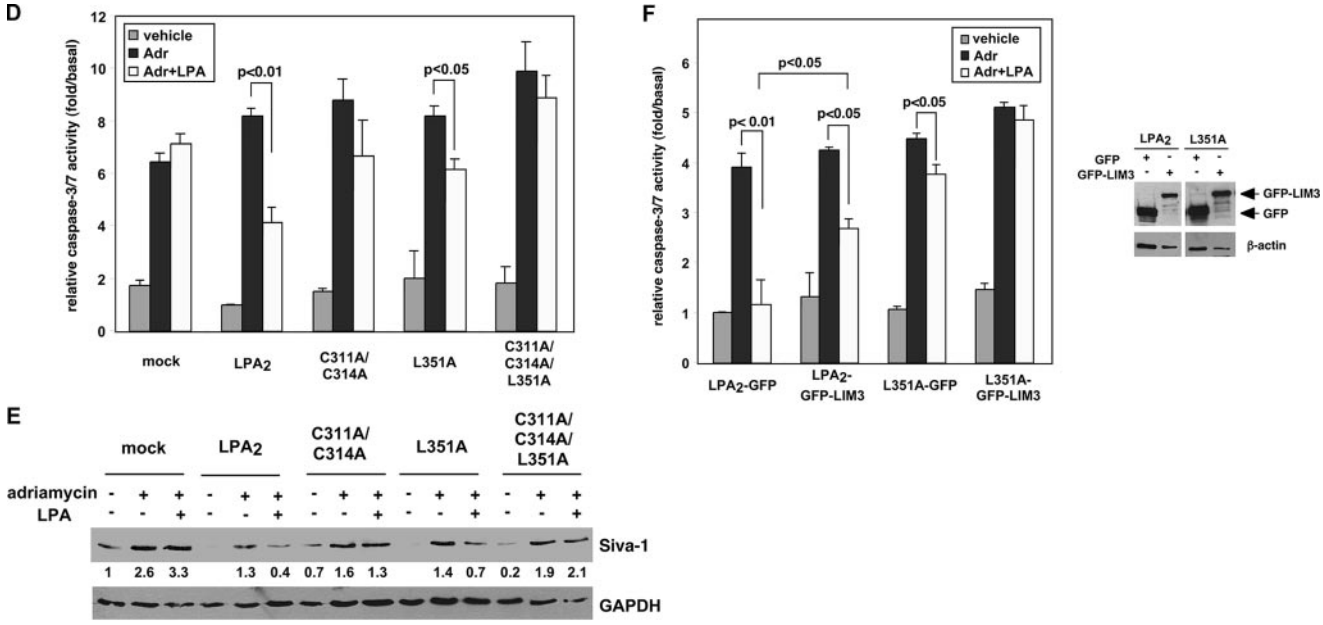

FIGURE 5—*continued*

A CXXC Motif Unique to the C-terminal Tail of LPA$_2$ Mediates the Interactions with TRIP6 and Siva-1—To investigate if the effects of these LPA$_2$-interacting partners on LPA-elicited chemoprotection are regulated through direct interactions with LPA$_2$, next we delineated the position of the TRIP6-interacting motif in the C terminus of LPA$_2$. We applied deletion mutagenesis while keeping the DSTL motif intact in the mutants to permit interactions with the PDZ partners. Cellular co-immunoprecipitation demonstrated that except for Δ309+DSTL, Δ302+DSTL, and Δ296 mutants, other deletion mutants of LPA$_2$, including Δ316+DSTL, Δ327+DSTL, Δ338+DSTL, Δ347, and Δ348, and the L351A point mutant that lacks PDZ binding were able to bind to TRIP6, although to a lesser degree than the WT LPA$_2$ (Fig. 2*A*). This result indicates that the minimal sequences required for TRIP6 binding contain residues 297–316. Alanine scanning mutational analysis of the 297–316 region identified Cys-311 and Cys-314 as the residues required for the interaction with TRIP6 (Fig. 2*B*). *In vitro* binding assays confirmed that mutation of Cys-311 and/or Cys-314 to Ala abolished the direct binding of LPA$_2$-CT to TRIP6 (Fig. 2*C*).

Next we examined the interaction of Siva-1 with WT or cysteine mutants of LPA$_2$. We found that only when both Cys-311 and Cys-314 were mutated was the interaction with Siva-1 completely abolished *in vitro* (Fig. 3*A*) and in cells (Fig. 3*B*). However, this binding was not affected by L351A mutation (Fig. 3*B*).

Among the endothelial differentiation gene family lysophospholipid receptors, the C*XX*C motif is unique only to the LPA-

FIGURE 5. **Protein-protein interactions via the C*XX*C- and/or PDZ-binding motifs do not affect LPA$_2$-mediated Ca^{2+} response but regulate its chemoprotective effect.** *A*, stable expression of LPA$_2$ or one of the point mutants deficient in binding to the zinc finger proteins and/or PDZ proteins in LPA$_{1/2}$ DKO MEFs. Total mRNAs were isolated from LPA$_1$ KO MEFs or one of the LPA$_{1/2}$ DKO MEF cell lines (mock, WT LPA$_2$, C311A/C314A, L351A, or C3131A/C314A/L351A). Quantitative real-time reverse transcriptase-PCR was performed to determine the relative expression levels of LPA$_2$ mRNA compared with that expressed in LPA$_1$ KO MEFs and was normalized by the expression of β-actin mRNA. Results show the mean ± S.E. done in triplicates and are representative of two separate experiments. To determine total protein levels of each receptor, FLAG-LPA$_2$ in the whole cell lysates was immunoprecipitated using anti-FLAG M2 monoclonal antibody-conjugated agarose beads and detected with an anti-FLAG rabbit polyclonal antibody. The result shown is representative of five independent experiments. *B*, mutation of the C*XX*C motif and/or PDZ-binding motif does not affect LPA$_2$-mediated Ca^{2+} response. Stable LPA$_{1/2}$ DKO MEFs were stimulated with different concentrations of LPA as indicated for 5 min. LPA-induced calcium response was determined as described previously (7). The curves for WT LPA$_2$ and mutants were generated by normalizing the Ca^{2+} peak at various dilutions to the response elicited by the highest concentration of LPA (1 μM) applied. The values of the mock-transduced MEFs were normalized to that of WT LPA$_2$-transduced MEFs. Data shown are the mean ± S.D. done in triplicates and are representative of two separate experiments. *C*, mutation of the C*XX*C motif and/or PDZ-binding motif attenuates LPA$_2$-mediated activation of ERK and AKT. Stable LPA$_{1/2}$ DKO MEFs were stimulated with LPA for 10 min. Immunoblotting was performed to detect the levels of phosphorylated and total ERK and AKT (*left panel*). The intensity of each protein was quantified to determine the relative activation fold of phospho-ERK and AKT by LPA stimulation (*right panel*). Data shown are the mean ± S.E. of five independent experiments. *, $p < 0.001$; **, $p < 0.01$; ***, $p < 0.05$ *versus* LPA-stimulated DKO-LPA$_2$ MEFs (Student's *t test*). *D*, LPA-mediated protection from adriamycin-induced caspase-3/7 activation is inhibited by mutation of both C*XX*C- and PDZ-binding motifs. Different LPA$_{1/2}$ DKO MEFs transfectants were pretreated with 10 μM LPA in 0.1% fatty acid-free BSA-containing medium for 1 h, followed by addition of 1.7 μM adriamycin for 8 h. Apoptosis was determined by caspase-3/7 activity assay. Data show the mean ± S.E. of four independent experiments. *E*, mutation of the C*XX*C motif abrogates LPA$_2$-mediated protection from adriamycin-induced Siva-1 induction. Different LPA$_{1/2}$ DKO MEFs were pretreated with 10 μM LPA for 2 h, followed by the addition of 1.5 μM adriamycin for 14 h. Immunoblotting (*IB*) was performed to detect the expression of Siva-1 and glyceraldehyde-3-phosphate dehydrogenase (*GAPDH*) in the whole cell lysates. The relative expression of Siva-1 was compared with that expressed in the mock cells without any treatment and was normalized by the levels of GAPDH. The result shown is representative of three independent experiments. *F*, inhibition of the C*XX*C motif-mediated interaction with TRIP6-LIM3 attenuates LPA-mediated protection from adriamycin-induced apoptosis. pEGFP or pEGFP-TRIP6-LIM3 was transiently transfected by electroporation into LPA$_{1/2}$ DKO MEFs that expressed WT LPA$_2$ or L351A. Cells were treated with 10 μM LPA for 1 h followed by addition of 1.5 μM adriamycin for 9 h. Caspase-3/7 activity was determined and normalized by protein concentrations in each sample. Data show the mean ± S.E. of three independent experiments. The immunoblot shows the expression of GFP-TRIP6-LIM3, GFP, and β-actin in the whole cell lysates.

specific LPA_2 and sphingosine 1-phosphate (S1P)-specific $S1P_1$ and $S1P_4$ receptors (Fig. 3*C*). In contrast to LPA_2, LPA_1 and LPA_3 lack the C*XX*C motif in the C terminus (Fig. 3*C*) and fail to interact with TRIP6 and Siva-1 (17, 18). $S1P_4$ formed a complex with Siva-1 but barely bound to TRIP6; and $S1P_1$, albeit weakly, associated with TRIP6 but not Siva-1 (Fig. 3, *D* and *E*). Thus, the C*XX*C motifs of distinct endothelial differentiation gene family lysophospholipid receptors are capable of mediating interactions with the C-terminal zinc finger of Siva-1 or TRIP6-LIM3 (Fig. 3*C*), which have been shown as the LPA_2-interacting domains (17, 18); however, additional residues are required for strengthening the interactions.

Previously we have demonstrated in NIH3T3 fibroblasts that Siva-1 colocalizes with LPA_2 in the cytosol and the plasma membrane, and this association prevents nuclear translocation of Siva-1 (18). Likewise, Siva-1 colocalized with LPA_2 and $S1P_4$ but not $S1P_1$ in the cytosol in $LPA_{1/2}$ DKO MEFs (Fig. 3*F*). When both Cys-311 and Cys-314 of LPA_2 were mutated to Ala, colocalization was completely abolished and Siva-1 was found in the nucleus.

Palmitoylation of LPA$_2$ Does Not Affect Its Ability to Interact with TRIP6, Siva-1, or NHERF2—Many GPCRs undergo cysteine palmitoylation that may affect their coupling to G proteins, cell surface receptor expression, receptor desensitization, or trafficking (23). However, the role of palmitoylation varies among different GPCRs. Among the several cysteine residues located in the C-terminal tail of LPA_2, including Cys-297, Cys-311, Cys-312, and Cys-314, mutation of a single cysteine residue either did not or slightly reduced palmitoylation of LPA_2 (Fig. 4*A*). Mutation of two or three cysteine residues partially reduced receptor palmitoylation but did not completely abolish this modification (Fig. 4*A*).

To evaluate whether palmitoylation affects LPA_2 binding to

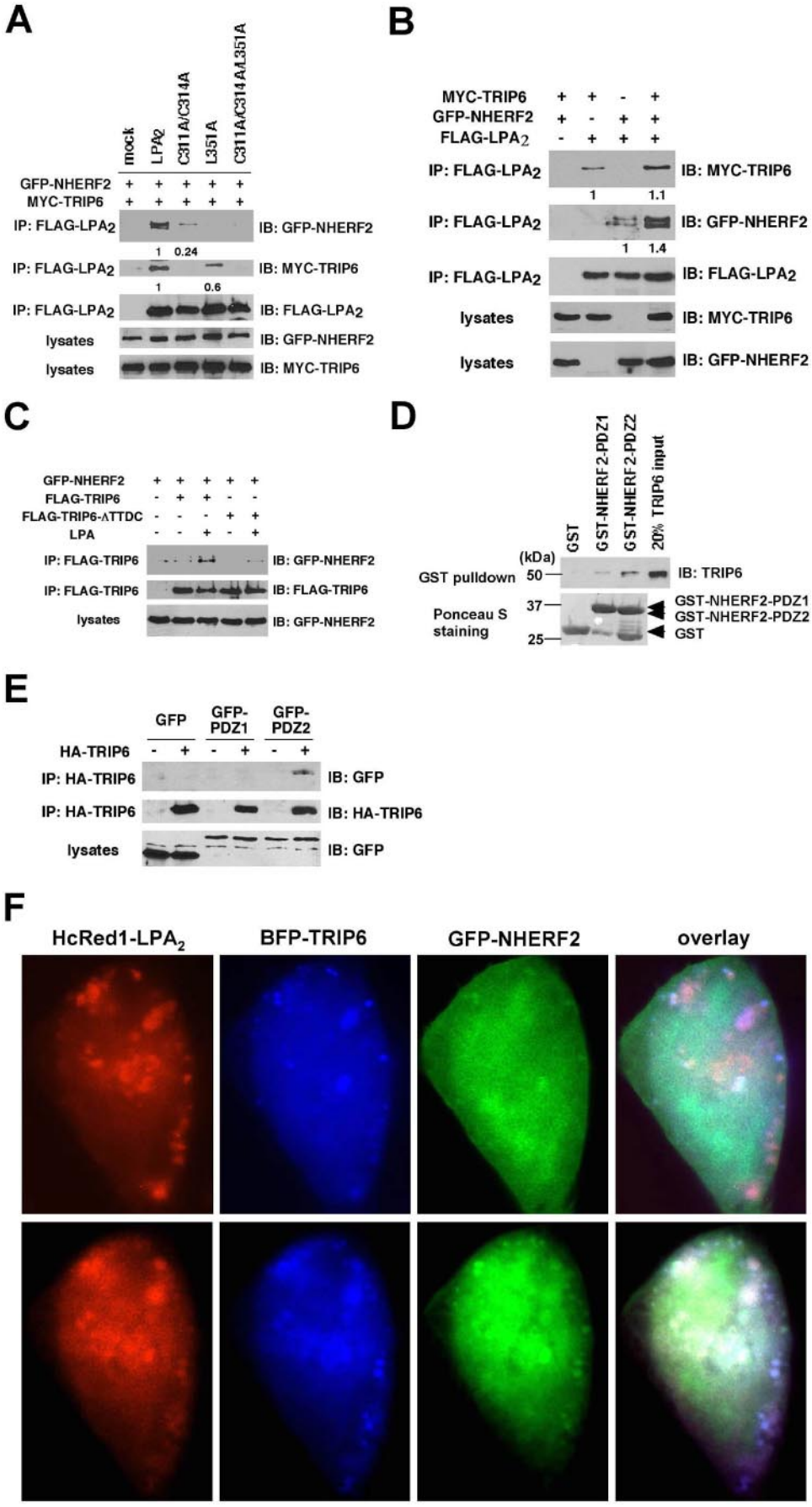

TRIP6, Siva-1, or NHERF2, we used 2-bromopalmitate to block palmitoylation and examined these interactions. Although 2-bromopalmitate inhibits palmitoylation of LPA_2 as assayed by determining the levels of palmitoylated LPA_2 with the acyl-biotinyl exchange procedure (22) and metabolic labeling of the receptor with [^{3}H]palmitic acid, it did not significantly affect interactions of LPA_2 with TRIP6, Siva-1, or NHERF2 (Fig. 4*B*).

G Protein-mediated LPA$_2$ Signaling to Calcium Mobilization Is Not Affected by Mutation of the CXXC- and/or PDZ-binding Motifs—To investigate the impact of mutations of the C-terminal binding motifs on LPA_2 functions, lentiviral constructs harboring WT LPA_2, the C311A/C314A mutant that is unable to interact with TRIP6 and Siva-1, the L351A mutant defective in binding to PDZ proteins, or the C311A/C314A/L351A mutant that cannot bind any of the interacting partners were stably transduced into the $LPA_{1/2}$ DKO MEFs. Compared with the endogenous LPA_2 mRNA expressed in the *LPA$_1$*$^{-/-}$ MEFs, the WT and point mutants of LPA_2 mRNA were expressed at 2.5- to 3-fold higher but comparable levels in the stable $LPA_{1/2}$ DKO MEF cell lines (Fig. 5*A*). They were also expressed at similar protein levels in the whole cell lysates (Fig. 5*A*) and on the cell surface demonstrated by flow cytometry analysis (data not shown). LPA-induced Ca^{2+} mobilization showed indistinguishable dose-response curves in the MEFs expressing WT or in any of the LPA_2 mutants (Fig. 5*B*), indicating that these binding motifs do not affect the $G_{q/11}$ signaling branch. These findings also imply that $G_{q/11}$-mediated signaling events are not altered by disruption of the palmitoylation modification of Cys-311 and Cys-314.

LPA$_2$-mediated Chemoprotection Is Attenuated by Mutation of the CXXC- and PDZ-binding Motifs—We reasoned that if LPA_2-mediated chemoprotection is regulated by these interacting partners, disruption of the interactions in itself would eliminate the function of TRIP6 and NHERF2 in promoting LPA_2-mediated prosurvival signaling and allow the stabilization of Siva-1, which can enhance chemotherapeutic agent-induced apoptosis. Indeed, the efficacy of LPA_2 in mediating LPA-induced ERK and AKT activation was significantly attenuated by C311A/C314A or L351A mutation and was completely abolished by the C311A/C314A/L351A mutation (Fig. 5*C*). These results suggest that the C*XX*C- and PDZ-binding motifs cooperatively regulate LPA_2-mediated prosurvival signaling.

Next we examined the effect of LPA on protecting adriamycin-induced apoptosis in these MEFs. The DNA fragmentation assay showed that following a 6-h adriamycin treatment, LPA protected cells from apoptosis in the $LPA_{1/2}$ DKO MEFs that expressed WT LPA_2, C311A/C314A, or L351A but not in the mock-transfected $LPA_{1/2}$ DKO MEFs or those expressing the C311A/C314A/L351A mutant (supplemental Fig. S1*A*). After an 8-h treatment, the antiapoptotic efficacy of LPA_2 measured by the caspase-3/7 activity assay (Fig. 5*D*) was reduced by the C311A/C314A or L351A mutations and was completely abolished by the C311A/C314A/L351A mutation. A similar effect was also observed using annexin V staining after a 14-h treatment (supplemental Fig. S1*B*).

Previously we have shown that LPA inhibits adriamycin-induced Siva-1 expression and its proapoptotic functions. Analysis of these LPA_2 mutants showed that the inhibitory effect of LPA on adriamycin-induced Siva-1 expression was eliminated by mutation of the C*XX*C motif but not the PDZ-binding motif, confirming that this regulation is mediated through the direct interaction of LPA_2 with Siva-1 (Fig. 5*E*). Together, these results suggest that the C*XX*C- and PDZ-binding motifs differentially and cooperatively regulate LPA_2 function in protecting cells from adriamycin-induced apoptosis.

The role of Siva-1 in apoptosis is well established (18); however, TRIP6 has not yet been implicated in antiapoptotic signaling and for this reason we focused our investigation on this adapter protein. The LIM3 domain of TRIP6 binds to LPA_2, and has been shown to serve as a dominant-negative probe to attenuate LPA_2-mediated cell migration previously (17). Overexpression of the GFP-TRIP6-LIM3 mutant reduced the chemoprotective effect of LPA in the DKO-LPA_2 MEFs, and this inhibitory effect was augmented in the DKO-L351A MEFs (Fig. 5*F*), supporting the notion that cooperative protein-protein interactions via both C*XX*C- and PDZ-binding motifs are required for the maximal protective effect of LPA_2. NHERF2 binds to LPA_2 through its PDZ2 domain (10). However, we did not succeed in overexpressing NHERF2-PDZ2 to attenuate the protective effect of LPA (data not shown).

FIGURE 6. **A PDZ-mediated association of TRIP6 and NHERF2 facilitates their interactions with LPA$_2$.** *A*, mutation of the C*XX*C (PDZ-binding) motif of LPA_2 abolishes the binding to TRIP6 (*NHERF2*) and also reduces the association with NHERF2 (*TRIP6*). GFP-NHERF2 and MYC-TRIP6 were coexpressed with WT or one of the mutants of FLAG-LPA_2 in HEK 293T cells. Co-immunoprecipitation (*IP*) was performed as described above. The relative levels of co-immunoprecipitated TRIP6 or NHERF2 were quantified and normalized to the immunoprecipitated WT or mutant of LPA_2. *B*, overexpression of TRIP6 enhances association of NHERF2 with LPA_2, and vice versa. FLAG-LPA_2 was co-expressed with MYC-TRIP6 and/or GFP-NHERF2 in HEK 293T cells as indicated. After stimulation of the cells with 2 μM LPA for 10 min, co-immunoprecipitation was performed. GFP-NHERF2 and MYC-TRIP6 co-immunoprecipitated with FLAG-LPA_2 were detected with an anti-GFP antibody and an anti-MYC antibody, respectively. The blot was reprobed with an anti-FLAG antibody to detect the immunoprecipitated LPA_2. The relative levels of co-immunoprecipitated TRIP6 or NHERF2 were quantified and normalized to the immunoprecipitated FLAG-LPA_2. *C*, C-terminal TTDC sequences of TRIP6 mediate the binding to NEHRF2. FLAG-TRIP6 or FLAG-TRIP6-ΔTTDC mutant lacking the C-terminal PDZ-binding motif was co-expressed with GFP-NHERF2 in HEK 293T cells. After stimulation of the cells with LPA for 10 min, WT or the ΔTTDC mutant of TRIP6 was immunoprecipitated with anti-FLAG M2 mouse monoclonal antibody-conjugated agarose beads and resolved by SDS-PAGE. Immunoblotting (*IB*) was performed using the antibodies specific to GFP and the FLAG epitope to detect GFP-NHERF2 and FLAG-TRIP6, respectively. *D*, TRIP6 binds to the PDZ domain of NHERF2 directly *in vitro*. Purified recombinant TRIP6 was incubated with GST, GST-NEHRF2-PDZ1, or GST-NHERF2-PDZ2 at 4 °C for 3 h. TRIP6 pulled down by glutathione *S*-transferase (*GST*) fusion proteins was detected by immunoblotting using an anti-TRIP6 antibody. The *bottom panel* shows expression of GST fusion proteins by Ponceau S staining. *E*, TRIP6 interacts with the PDZ2 but not PDZ1 domain of NHERF2 in cells. HA-TRIP6 was co-expressed with GFP, GFP-NHERF2-PDZ1, or GFP-NHERF2-PDZ2 in HEK 293T cells. TRIP6 in the whole cell lysates was immunoprecipitated with anti-HA mouse monoclonal antibody-conjugated agarose beads and resolved by SDS-PAGE. The immunoblot was probed with an anti-GFP antibody to detect GFP-NHERF2-PDZ2. The blot was reprobed with an anti-HA rabbit antibody to detect the immunoprecipitated HA-TRIP6. Data shown in each figure are representative of two to four independent experiments. *HA*, hemagglutinin. *F*, LPA_2, TRIP6, and NHERF2 colocalize in cells. Hc-Red1-LPA_2 was transiently co-expressed with BFP-TRIP6 and GFP-NHERF2 in $LPA_{1/2}$ DKO MEFs. Cells were starved for 1 h, followed by addition of 2 μM LPA for 10 min. Subcellular distribution of these molecules was visualized by fluorescence microscopy.

The results also showed that when $G_{i/o}$ signaling was inhibited with PTX, LPA-mediated ERK activation and protection from adriamycin-induced apoptosis were partially attenuated in DKO-LPA$_2$ MEFs (supplemental Fig. S2), suggesting that $G_{i/o}$ signaling to some extent is involved in the LPA$_2$-mediated antiapoptotic signaling. Nonetheless, LPA-induced recruitment of Siva-1, TRIP6, or NHERF2 was not significantly altered by treatment with PTX or the U73122 phospholipase C inhibitor (supplemental Fig. S3, *A* and *B*), suggesting that the macromolecular complex formation via the C terminus of LPA$_2$ is independent on $G_{i/o}$ or $G_{q/11}$ signaling.

The PDZ-mediated Association of TRIP6 with NHERF2 Facilitates Their Interaction with LPA$_2$—When we examined the interaction of different LPA$_2$ mutants with TRIP6 or NHERF2, we noticed that the C311A/C314A mutant, which does not bind to TRIP6, also showed reduced association with NHERF2 compared with WT LPA$_2$ (Fig. 6*A*). Likewise, the L351A mutant defective in binding to NHERF2 showed reduced association with TRIP6 (Fig. 6*A*) but not Siva-1 (Fig. 3*B*). Conversely, the interaction of NHERF2 or TRIP6 with LPA$_2$ was further enhanced when all three proteins were overexpressed (Fig. 6*B*). TRIP6 contains a C-terminal TTDC PDZ-binding motif, potentially allowing it to interact with PDZ proteins, raising the possibility that cooperativity might exist between TRIP6 and NHERF2 in interacting with LPA$_2$. Indeed, we found LPA induced the association of NHERF2 with TRIP6 but not the TRIP6-ΔTTDC mutant in HEK 293T cells (Fig. 6*C*). Domain mapping confirmed that TRIP6 preferentially binds to PDZ2 but not PDZ1 of NHERF2 *in vitro* (Fig. 6*D*) and also in HEK 293T cells (Fig. 6*E*). Because both LPA$_2$ and TRIP6 bind to the PDZ2 domain of NHERF2, NHERF2 must be present in dimer form to bridge LPA$_2$ and TRIP6. In

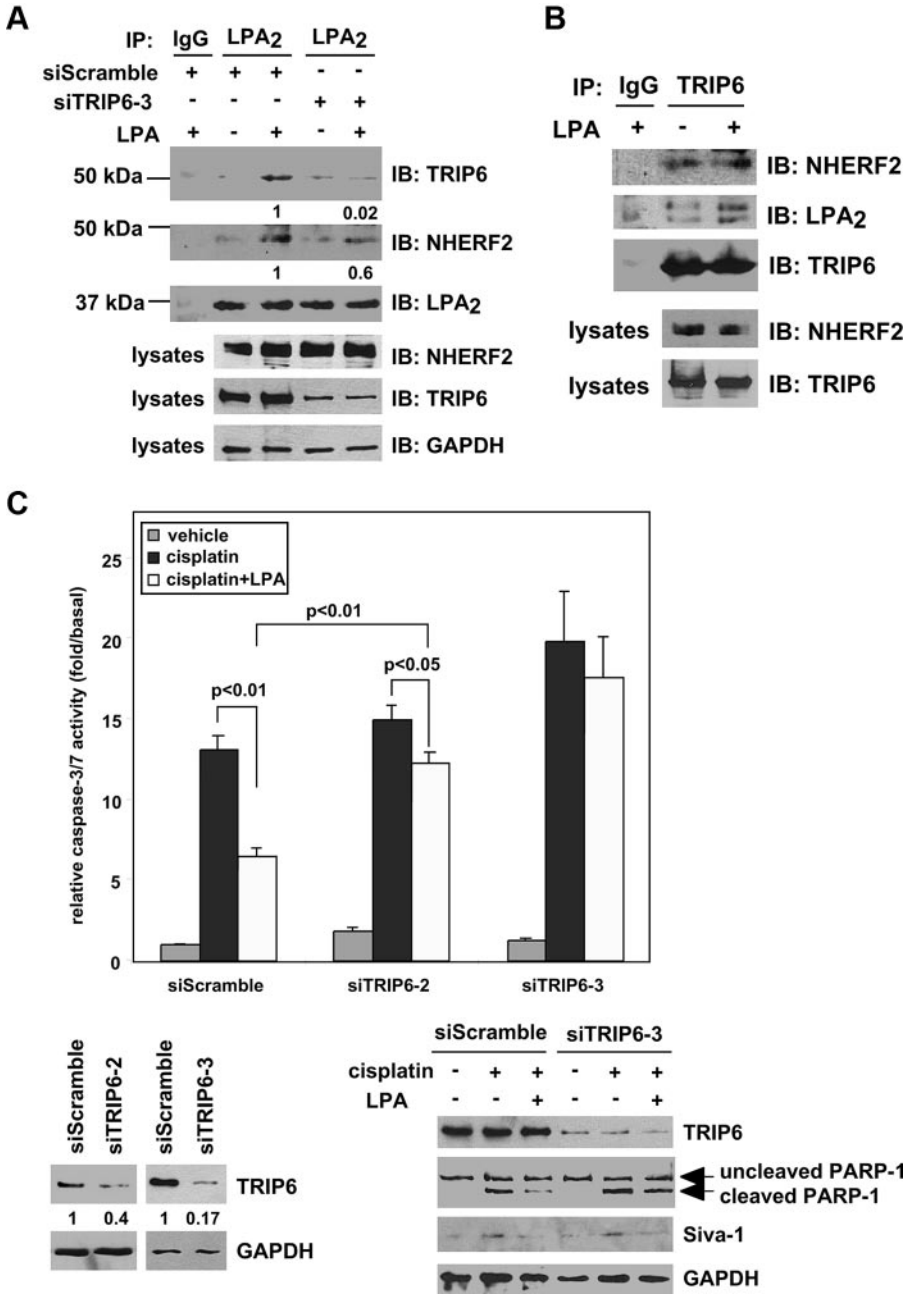

FIGURE 7. **Endogenous TRIP6 and NHERF2 form a ternary complex with LPA$_2$ by LPA stimulation, and regulate LPA-mediated chemoprotection in SKOV-3 cells.** *A*, inhibition of TRIP6 expression reduces LPA-induced association of NHERF2 with LPA$_2$. SKOV-3 cells expressing a scrambled siRNA or a TRIP6 siRNA (*siTRIP6-3*) were starved overnight followed by treatment with 2 μM LPA for 10 min. LPA$_2$ in the whole cell lysates was immunoprecipitated (*IP*) with an anti-LPA$_2$ rat antibody or a control IgG and resolved by SDS-PAGE. Immunoblotting (*IB*) was performed using the antibodies specific to NHERF2, TRIP6, and LPA$_2$, respectively. The *bottom three panels* show expression of NHERF2, TRIP6, and control glyceraldehyde-3-phosphate dehydrogenase (*GAPDH*) in the whole cell lysates. The relative levels of co-immunoprecipitated TRIP6 or NHERF2 were quantified and normalized to the immunoprecipitated FLAG-LPA$_2$. *B*, TRIP6 interacts with NHERF2 constitutively in SKOV-3 cells. SKOV-3 cells were treated with LPA as described in *A*. TRIP6 in the whole cell lysates was immunoprecipitated with an anti-TRIP6 mouse monoclonal antibody or a control IgG. After SDS-PAGE, the immunoblot was probed with an anti-NHERF2 antibody, an anti-LPA$_2$ antibody followed by an anti-TRIP6 antibody. Results shown in *A* and *B* are representative of three independent experiments. *C* and *D*, LPA-mediated protection of SKOV-3 cells from cisplatin-induced apoptosis is eliminated by knockdown of TRIP6 or NHERF2 expression. SKOV-3 cells expressing a scrambled siRNA or one of the siRNAs that specifically target human TRIP6 (*siTRIP6-2* and *siTRIP6-3*) (*C*) or NHERF2 (siNHERF2–4, siNHERF2–5) (*D*) as indicated were pretreated with 10 μM LPA for 1 h followed by the addition of 50 μM cisplatin for 20 h. Caspase-3/7 activity was determined. Data shown are the mean ± S.E. of three independent experiments. The knockdown effect of each TRIP6 siRNA or NHERF2 siRNA was determined by immunoblotting using an antibody specific to TRIP6 or NHERF2, respectively. Half of the lysates as indicated were subjected to immunoblotting using the antibodies specific to PARP-1, Siva-1, NHERF2, and GAPDH, respectively. *E*, a model for the regulation of LPA$_2$-mediated antiapoptotic signaling through the *CXXC*-mediated interaction with Siva-1, and the *CXXC*- and PDZ-mediated LPA$_2$-TRIP6-NHERF2 ternary complex formation.

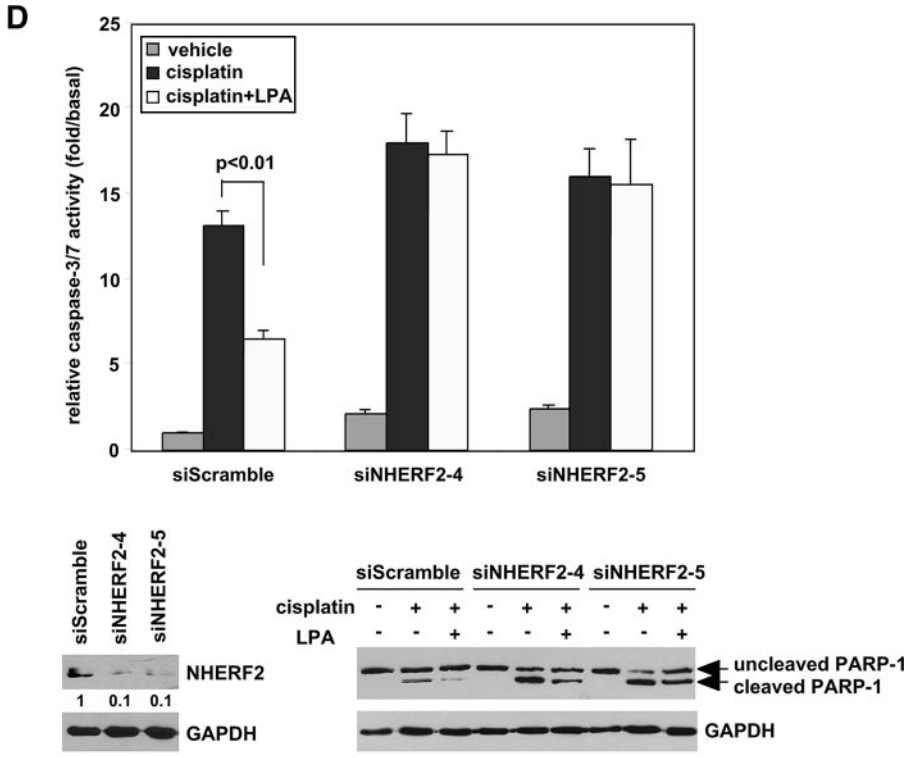

FIGURE 7—*continued*

support of this notion, it is known that NHERF2 forms oligomers through PDZ1- and/or PDZ2-mediated self-association (24).

To address whether LPA_2, TRIP6, and NHERF2 are present in the same macromolecular complex, fluorescence microscopy was performed to examine subcellular distribution of these molecules. We found that HcRed1-LPA_2, BFP-TRIP6, and GFP-NHERF2 formed clusters and colocalized in close proximity to the plasma membrane or inside the cytosol after LPA treatment for 10 min (Fig. 6*F*). Together, these results suggest that LPA_2 forms a ternary macromolecular complex with TRIP6 and NHERF2 by LPA stimulation.

TRIP6 and NHERF2 Regulate LPA-mediated Chemoprotection in Ovarian Cancer Cells—To understand the physiological relevance of NHERF2-TRIP6-LPA_2 ternary complex formation, co-immunoprecipitation was performed in SKOV-3 cells that express high levels of these three proteins. LPA induced the association of LPA_2 with both TRIP6 and NHERF2 at physiological levels (Fig. 7*A*). When TRIP6 expression was knocked down, the interaction of NHERF2 with LPA_2 was significantly attenuated, suggesting that TRIP6 facilitates this association. However, the association of TRIP6 with LPA_2 was not significantly altered by knockdown of NHERF2 expression (supplemental Fig. S4), perhaps because either TRIP6 binds to LPA_2 with a higher affinity or other LPA_2-interacting PDZ proteins can also facilitate the association of TRIP6 with LPA_2. In SKOV-3 cells, TRIP6 associated with NHERF2 constitutively. Nonetheless, formation of the ternary complex required LPA stimulation (Fig. 7*B*).

LPA also protected cells from cisplatin-induced caspase-3/7 activation and PARP-1 cleavage in SKOV-3 ovarian cancer cells (Fig. 7*C*). We found 60% knockdown of TRIP6 expression attenuated LPA-mediated chemoprotection in SKOV-3 cells (Fig. 7*C*) as that shown in DKO-LPA_2 MEFs (Fig. 1*A*). When TRIP6 expression was knocked down by 80–90%, the protective effect of LPA on cisplatin-induced caspase-3/7 activation and PARP-1 cleavage was almost completely eliminated (Fig. 7*C*). A similar effect was found by 90% knockdown of NHERF2 expression (Fig. 7*D*). Together, these results suggest that both TRIP6 and NHERF2 play a significant role in the LPA-mediated antiapoptotic effect in SKOV-3 cells. Lacking functional p53, cisplatin only induced modest Siva-1 expression in SKOV-3 cells (Fig. 7*C*). Although both TRIP6 and Siva-1 bind to the C*XX*C motif of LPA_2, knockdown of TRIP6 expression did not alter the effect of LPA on reducing Siva-1 expression.

In summary, these data suggest that LPA induces the formation of a ternary complex containing LPA_2, TRIP6, and NHERF2. Our results favor the model that in addition to binding to Siva-1 and down-regulating its activity, LPA_2 forms a supramolecular complex with TRIP6 and NHERF2. Together, they coordinately regulate the antiapoptotic signaling of LPA_2 (Fig. 7*E*).

DISCUSSION

GPCRs are increasingly viewed as a nidus for generating ligand-activated intracellular signals via interactions with G proteins and non-G protein signaling molecules (25, 26). We hypothesized that the macromolecular complex formed via the unique C-terminal binding motifs of LPA$_2$ could be responsible for its antiapoptotic function. This hypothesis was based in part on the high degree of sequence diversity in the C termini of the endothelial differentiation gene family LPA receptors, which show only seven of 55 residues are conserved in the C terminus, in contrast to the 85% homology in their transmembrane domains. In support of this hypothesis, it has been shown that PDZ proteins, including NHERF2, interact with the C-terminal DSTL motif of LPA$_2$ but not with other LPA receptor subtypes (10, 12, 13). Moreover, LPA$_2$ is the only LPA receptor subtype that interacts with Siva-1 and TRIP6 (17, 18).

Using the LPA$_{1/2}$ DKO MEFs that stably express a human LPA$_2$ as the model system, we present evidence that siRNA-mediated knockdown of TRIP6 or NHERF2 expression attenuates LPA$_2$-mediated chemoprotection; in contrast, knockdown of Siva-1 enhances this effect. We have mapped the ^{311}C*XX*C^{314} motif of LPA$_2$ required for interactions with TRIP6 and Siva-1, and demonstrated that disruption of either the C*XX*C motif or PDZ-binding motif attenuated LPA$_2$-mediated chemoprotection, and only when both binding motifs were disrupted, it completely abolished this effect. Together, these data indicate that LPA$_2$-mediated chemoprotection is regulated through these supramolecular complexes.

Palmitoylation of the four C-terminal cysteine residues of LPA$_2$ showed that those in the C*XX*C motif can be lipid-modified, however, inhibition of this modification did not disrupt interaction with TRIP6 or Siva-1, indicating that palmitoylation of LPA$_2$ is neither required nor preclusive for the interaction with TRIP6 or Siva-1. We also found that blocking $G_{i/o}$ protein activation with PTX or inhibiting $G_{q/11}$ signaling with the U73122 phospholipase C inhibitor did not affect the interaction of LPA$_2$ with Siva-1, TRIP6, or NHERF2, suggesting that G protein signaling is also not required for these protein interactions. On the other hand, mutation of the C*XX*C- or PDZ-binding motif of LPA$_2$ did not affect $G_{q/11}$-mediated Ca^{2+} transients upon LPA stimulation, indicating that these binding motifs do not affect the $G_{q/11}$ signaling branch.

Unexpectedly, we found that truncation or point mutations that abolish the interactions of LPA$_2$ with PDZ proteins also attenuated the binding of TRIP6 to LPA$_2$. These observations led us to hypothesize that cooperativity might exist between TRIP6 and NHERF2 in interacting with LPA$_2$. Indeed, we found evidence that TRIP6 interacts with the PDZ2 domain of NHERF2 via its C-terminal TTDC PDZ-binding motif. Overexpression of TRIP6 augments the complex formation between LPA$_2$ and NHERF2, whereas knockdown of TRIP6 diminishes it. Moreover, upon ligand activation LPA$_2$ colocalizes with both TRIP6 and NHERF2. Thus, it is likely that LPA$_2$, TRIP6, and NHERF2 form a ternary complex in the microdomain of the plasma membrane to coordinately regulate LPA$_2$-elicited chemoprotective effect. This complex appears to be assembled upon LPA stimulation in SKOV-3 cells at endogenous levels of the participating proteins. Our new data and previous reports (10, 12, 20, 27) show that both TRIP6 and NHERF2 are involved in LPA-induced ERK and AKT activation. SKOV-3 ovarian cancer cells show very low levels of phosphatase and tensin homolog but high activity of AKT (28, 29). When TRIP6 or NHERF2 was knocked down to a great extent, it almost completely eliminated LPA-mediated chemoprotection in SKOV-3 cells. Similarly, it has been reported that knockdown of NHERF2 expression abrogates the chemoprotective effect of LPA in colon cancer cells (27).

We also note that the C*XX*C motif is required for the antiapoptotic effect through the inhibition of Siva-1 signaling. However, Siva-1 interaction with LPA$_2$ does not appear to be affected by disruption of the LPA$_2$ interaction with PDZ proteins. Our data showed that PTX slightly attenuated LPA-induced chemoprotection, suggesting that $G_{i/o}$-mediated signals contribute to but are not sufficient for the full antiapoptotic effect of LPA$_2$. Assembly of the LPA$_2$-TRIP6-NHERF$_2$ ternary complex appears to play a fundamental role in the ability of LPA to render cancer cells resistant to chemotherapeutic agents as we have demonstrated for the case of adriamycin and cisplatin.

Taken together, these data point to a novel signal amplification/diversification mechanism originating from the GPCR signal transduction hub. We favor the hypothesis that signals from protein-protein interactions via the C-terminal C*XX*C- and PDZ-binding motifs are integrated with G protein-activated signals to cooperatively regulate the antiapoptotic function of LPA$_2$.

Acknowledgments—We thank Dr. Junken Aoki for providing the anti-LPA$_2$ antibody, Dr. A. P. Naren for the anti-NHERF2 antibody and pGEX-NHERF2, and Dr. Tim Towne for sharing the flow cytometry equipment.

REFERENCES

1. Mills, G. B., and Moolenaar, W. H. (2003) *Nat. Rev. Cancer* **3,** 582–591
2. Moolenaar, W. H., van Meeteren, L. A., and Giepmans, B. N. (2004) *Bioessays* **26,** 870–881
3. Parrill, A. L. (2008) *Biochim. Biophys. Acta* **1781,** 540–546
4. Pasternack, S. M., von Kugelgen, I., Aboud, K. A., Lee, Y. A., Ruschendorf, F., Voss, K., Hillmer, A. M., Molderings, G. J., Franz, T., Ramirez, A., Nurnberg, P., Nothen, M. M., and Betz, R. C. (2008) *Nat. Genet.* **40,** 329–334
5. Tabata, K., Baba, K., Shiraishi, A., Ito, M., and Fujita, N. (2007) *Biochem. Biophys. Res. Commun.* **363,** 861–866
6. Radeff-Huang, J., Seasholtz, T. M., Matteo, R. G., and Brown, J. H. (2004) *J. Cell Biochem.* **92,** 949–966
7. Deng, W., E, S., Tsukahara, R., Valentine, W. J., Durgam, G., Gududuru, V., Balazs, L., Manickam, V., Arsura, M., VanMiddlesworth, L., Johnson, L. R., Parrill, A. L., Miller, D. D., and Tigyi, G. (2007) *Gastroenterology* **132,** 1834–1851
8. Lin, F. T., and Lai, Y. J. (2008) *Biochim. Biophys. Acta* **1781,** 558–562
9. Li, C., Dandridge, K. S., Di, A., Marrs, K. L., Harris, E. L., Roy, K., Jackson, J. S., Makarova, N. V., Fujiwara, Y., Farrar, P. L., Nelson, D. J., Tigyi, G. J., and Naren, A. P. (2005) *J. Exp. Med.* **202,** 975–986
10. Oh, Y. S., Jo, N. W., Choi, J. W., Kim, H. S., Seo, S. W., Kang, K. O., Hwang, J. I., Heo, K., Kim, S. H., Kim, Y. H., Kim, I. H., Kim, J. H., Banno, Y., Ryu,

S. H., and Suh, P. G. (2004) *Mol. Cell Biol.* **24,** 5069–5079
11. Yamada, T., Ohoka, Y., Kogo, M., and Inagaki, S. (2005) *J. Biol. Chem.* **280,** 19358–19363
12. Yun, C. C., Sun, H., Wang, D., Rusovici, R., Castleberry, A., Hall, R. A., and Shim, H. (2005) *Am. J. Physiol.* **289,** C2–C11
13. Zhang, H., Wang, D., Sun, H., Hall, R. A., and Yun, C. C. (2007) *Cell. Signal.* **19,** 261–268
14. Takahashi, Y., Morales, F. C., Kreimann, E. L., and Georgescu, M. M. (2006) *EMBO J.* **25,** 910–920
15. Wu, Y., Dowbenko, D., Spencer, S., Laura, R., Lee, J., Gu, Q., and Lasky, L. A. (2000) *J. Biol. Chem.* **275,** 21477–21485
16. Chun, J., Kwon, T., Lee, E., Suh, P. G., Choi, E. J., and Sun Kang, S. (2002) *Biochem. Biophys. Res. Commun.* **298,** 207–215
17. Xu, J., Lai, Y. J., Lin, W. C., and Lin, F. T. (2004) *J. Biol. Chem.* **279,** 10459–10468
18. Lin, F. T., Lai, Y. J., Makarova, N., Tigyi, G., and Lin, W. C. (2007) *J. Biol. Chem.* **282,** 37759–37769
19. Bach, I. (2000) *Mech. Dev.* **91,** 5–17
20. Lai, Y. J., Chen, C. S., Lin, W. C., and Lin, F. T. (2005) *Mol. Cell. Biol.* **25,** 5859–5868
21. Fortin, A., MacLaurin, J. G., Arbour, N., Cregan, S. P., Kushwaha, N., Callaghan, S. M., Park, D. S., Albert, P. R., and Slack, R. S. (2004) *J. Biol. Chem.* **279,** 28706–28714
22. Wan, J., Roth, A. F., Bailey, A. O., and Davis, N. G. (2007) *Nat. Protoc.* **2,** 1573–1584
23. Qanbar, R., and Bouvier, M. (2003) *Pharmacol. Ther.* **97,** 1–33
24. Lau, A. G., and Hall, R. A. (2001) *Biochemistry* **40,** 8572–8580
25. Hur, E. M., and Kim, K. T. (2002) *Cell. Signal.* **14,** 397–405
26. Maudsley, S., Martin, B., and Luttrell, L. M. (2005) *J. Pharmacol. Exp. Ther.* **314,** 485–494
27. Rusovici, R., Ghaleb, A., Shim, H., Yang, V. W., and Yun, C. C. (2007) *Biochim. Biophys. Acta* **1770,** 1194–1203
28. Longva, K. E., Pedersen, N. M., Haslekas, C., Stang, E., and Madshus, I. H. (2005) *Int. J. Cancer* **116,** 359–367
29. Wang, H. Q., Altomare, D. A., Skele, K. L., Poulikakos, P. I., Kuhajda, F. P., Di Cristofano, A., and Testa, J. R. (2005) *Oncogene* **24,** 3574–3582